ChemPubSoc Europe

DOI: 10.1002/batt.201800078

BATTERIES & SUPERCAPS Communications

Suitability of Blended Ionic Liquid-Dimethylsulfoxide Electrolyte for Lithium-Oxygen Battery

Etienne Knipping,*[a, b] Christophe Aucher,[a] Gonzalo Guirado,[b] and Laurent Aubouy[a]

Electrolytes composed of dimethylsulfoxide (DMSO), 1-ethyl-3-methylimidazolium bis(trifluoromethylsulfonyl)imide (EMI TFSI) and $LiClO_4$ are characterized for application in lithium-oxygen batteries. The increase of EMI TFSI content in the electrolyte enables to improve its thermal stability and to decrease the overpotential of the cell. The optimum addition of EMI TFSI enables to reduce the overpotential from 1.43 V to 1.06 V, with a cyclability of 69 cycles with 600 mAh g^{-1} of limited capacity.

The Li-O_2 battery has received much interest in the last few years, as its theoretical capacity reaches 5–10 times the current Li-ion battery capacity.[1] The main electrochemical process in an aprotic Li–O_2 battery is the formation and decomposition of the Li_2O_2, during discharge and recharge respectively. However, this reaction suffers from low reversibility leading to a low cyclability of the battery. Recently, Room Temperature Ionic Liquids (RTILs) attracted much attention for Li–O_2 battery electrolyte.[2–12] Namely, Nakamoto et al.[13] demonstrated the advantage of the RTILs stability against electrochemical oxidation vs. Li^+/Li and O_2 redox reversibility. Cai et al.[14] proved that ionic liquid could show higher specific capacity compared to carbonate solvent electrolytes. Moreover, Cechetto et al.[15] observed a decrease of 0.4 V of the overpotential by mixing ionic liquids with an ether-based electrolyte. This could be explained by a higher ionic conductivity of the electrolyte containing the ionic liquid, a less insulating Li_2O_2 particle interface and a better Li_2O_2 solubility resulting to improved kinetics of the Li_2O_2 oxidation. On the other hand, pure RTIL electrolytes were tested in previous experiments, but an adequate reversibility of the Li–O_2 battery reaction is not attainable probably due to their high viscosity that affects the ion diffusion and the kinetics of the battery reaction.[16] Moreover, poor battery capacity[13] and a cyclability lower than 30 cycles is generally obtained.[5,14] In the present work, we study the influence of the 1-ethyl-3-methylimidazolium bis(trifluoromethylsulfonyl)imide (EMI TFSI) as co-solvent of Li-O_2 battery electrolyte in the final aim of designing an adequate solution for this technology. Thermal properties, stability with lithium metal and electrochemical performance are evaluated for DMSO-based electrolyte containing different amount of EMI TFSI, a RTIL known for its thermal resistance, high conductivity and electrochemical stability.[17] Hence, four mixed electrolytes ET-0, ET-30, ET-50 and ET-100 are prepared by adding 5 w% of $LiClO_4$ to the mixed solution of DMSO and EMI TFSI, the weight ratio of EMI TFSI/DMSO being 0/100, 30/70, 50/50 and 100/0 respectively. The results are summarized in the Table 1.

Table 1. Ionic conductivity, viscosity, degradation temperature, capacity, overpotential and cycling life of the four studied electrolytes.

	ET-0	ET-30	ET-50	ET-100
Ionic conductivity (mS cm^{-1})	7.88	13.1	10.1	0.49
Viscosity (cP)	6.5	6.3	12	81
Degradation temperature (°C)	105	182	>200	>200
Capacity full discharge (mAh g^{-1})	5651	7618	4631	3060
Overpotential 1st cycle (V)	1.43	1.06	0.90	1.16
Cycling life (cycles)	98	69	18	7

The effect of the use of ionic liquids on the thermal stability of the above-mentioned electrolytes are analyzed by performing DSC tests. Before the heating ramp, the samples are cooled and equilibrated at −90 °C to allow their crystallization. In the case of ET-0 and ET-30, the DSC profiles (Figure 1) show endothermic peaks at 13 and 2 °C respectively, corresponding to the melting point. The ET-0 shows another endothermic peak at −7 °C that may correspond to a solid-solid phase transition. For the samples with more EMI TFSI content, i.e. ET-50 and ET-100, no crystalline phase is detected, showing that for the procedure used, the electrolytes remained amorphous.

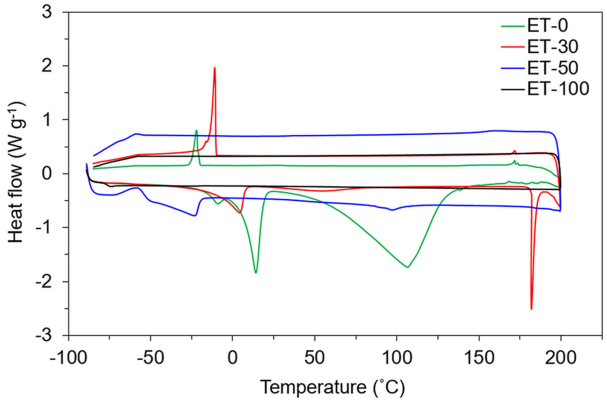

Figure 1. DSC profiles of the ET-0, ET-30, ET-50 and ET-100 electrolytes.

[a] Dr. E. Knipping, Dr. C. Aucher, Dr. L. Aubouy
Leitat Technological Center
Carrer de la Innovació 2, 08225 Terrassa, Spain
E-mail: eknipping@leitat.org
[b] Dr. E. Knipping, Dr. G. Guirado
Departament de Química
Universitat Autònoma de Barcelona
E-08193 Bellaterra, Barcelona, Spain

Moreover, thermal stability is improved with the addition of EMI TFSI. Without RTIL, an endothermic peak occurred at 105 °C, corresponding to the evaporation of the DMSO. However, when 30% of EMITFSI is added, the endothermic peak is postponed to 182 °C. For ET-50 and ET-100, no endothermic peak is observed, showing that the degradation of the electrolyte occurs at higher temperature. The safety of the battery can be then improved with the addition of an RTIL, as it can enhance the thermal stability of the electrolyte.

Ionic conductivity and viscosity of the blended electrolytes are measured and represented in function of the DMSO/EMI TFSI ratio (Figure 2). The ionic conductivity initially increases with increasing EMI TFSI content, reaching a maximum of 13.1 mS cm^{-1} at 30% by weight. Because EMI TFSI itself is a salt, the number of ions in the electrolyte increases with increasing EMI TFSI content and then the ionic conductivity too. However, adding EMI TFSI increases also the viscosity of the electrolyte from 6.5 cP for ET-0 to 81.4 for ET-100, due to the increased ion-solvent interactions and Coulombic interactions between ionic species.[8] Thus, the decrease of the ionic conductivity from 50% of EMI TFSI content can be attributed to the increase of the viscosity. It is shown then that the addition of a small amount of RTIL in the electrolyte can increase its ionic conductivity, which may be beneficial for the battery.

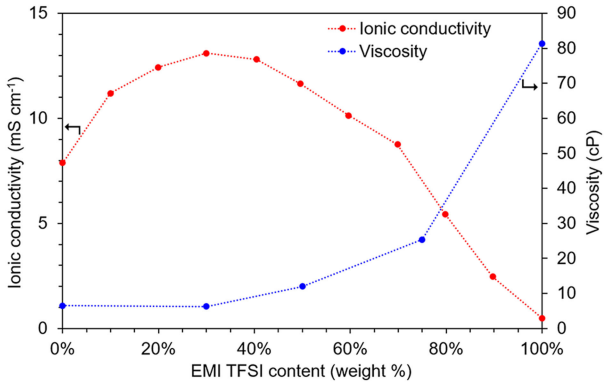

Figure 2. Ionic conductivity and viscosity of blended electrolytes as function of EMI TFSI content in the EMI TFSI/DMSO solution. All the solutions have $LiClO_4$ content of 5 wt%.

To verify the compatibility of these new electrolytes with the lithium anode, Li/Li stripping/plating test is realized within the different electrolyte at 10 mA cm^{-2} and 25 °C. The cell is charged at constant current for 1 hour at 10 mA cm^{-2} and subsequently discharge for 1 hour at −10 mA cm^{-2}. A typical voltage profile is shown in the Figure 3-A. Since the cell is symmetric, it is not affected by parasitic chemical or electrochemical reactions and the cycles are symmetrical.[18,19] The evolution of the overpotential of the Li/Li cell is shown for each electrolyte (Figure 3-B). With the ET-0 as electrolyte, the cell voltage is seen to be very low, around 9 mV vs. Li$^+$/Li and stays constant upon cycling for at least 200 cycles. This low voltage amplitude confirms that no stable passivation layer is formed.[20] Concerning both blended electrolytes (ET-30 and ET-50), the cell voltage varies between 0.2 and 0.5 V vs. Li$^+$/Li, which is due to the formation of a solid electrolyte interphase (SEI) layer. A cell voltage around 0.1 V vs. Li$^+$/Li for ET-100 is observed, showing that the lithium surface is passivated in the presence of the EMI TFSI, probably due to molecule adsorption at the surface within lower voltage amplitude with respect to blended electrolytes. In all cases, the electrolyte enables the stripping/plating of the lithium.

The full discharge capacities of the Li-O_2 cells were measured at a constant specific current of 200 mA g^{-1}. The first full discharge curves obtained with the different electrolytes are shown in the Figure 4. The cell with ET-30 presents the highest capacity with 7618 mAh g^{-1}, whereas the cell with RTIL-free electrolyte (ET-0) has a capacity of 5651 mAh g^{-1}. This improvement by adding 30% of EMI TFSI can be explained by the higher ionic conductivity and a better wettability of the ET-30. Indeed, the EMI TFSI, which is hydrophobic, may have more affinity with the hydrophobic carbon.[8] However, adding more EMI TFSI in the electrolyte increases the viscosity, which leads to lower capacity. An optimization of the electrolyte content is then needed to achieve high battery performance. The four

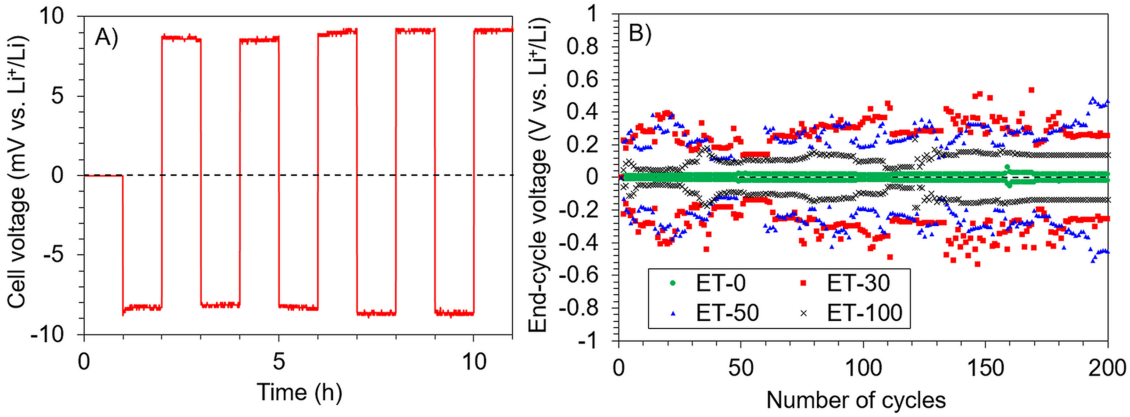

Figure 3. A) Typical voltage behavior of Li–Li cell during galvanostatic lithium stripping/plating cycle test (case of ET-0). A current of 10 mA cm^{-2} was applied for 1 hour in each direction. B) Evolution of the cell-voltage cutoff with the number of cycles for the different electrolytes studied

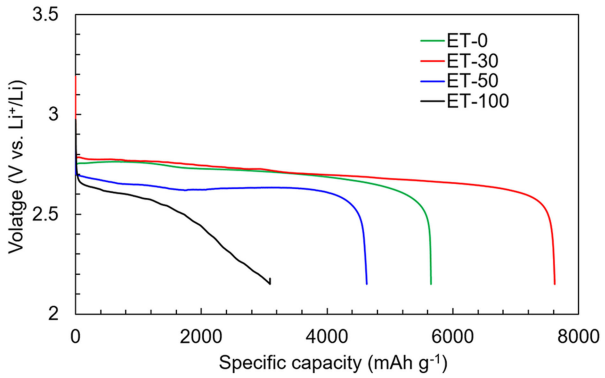

Figure 4. Initial full discharge curves of Li–O_2 cells at 25 °C with ET-0, ET-30, ET-50 and ET-100 electrolytes.

electrolytes are then tested in Li–O_2 cells to obtain discharge/recharge cycles at a controlled depth of discharge of 600 mAh g^{-1} and constant current of 200 mA g^{-1}. On the first cycle (Figure 5), the oxidation potential decreases with increased content of EMI TFSI. Indeed, the higher ionic conductivity of ET-30 and ET-50 compared to ET-0 enables faster kinetics of the oxidation reactions. The difference between ET-30 and ET-50, 3.86 and 3.68 V vs. Li^+/Li respectively, may be ascribed to a better wettability of the ET-50 electrolyte.[8] The higher EMI TFSI content makes the electrolyte more hydrophobic, wetting then more effectively the hydrophobic carbon cathode. Concerning the ET-100, the discharge plateau has a lower voltage (2.66 V vs. Li^+/Li) than for the electrolytes containing DMSO (2.80 V vs. Li^+/Li). Despite its high viscosity, the ET-100 show low oxidation potential of only 3.82 V vs. Li^+/Li, which may be due its hydrophobicity.[8] However, this oxidation potential is higher than for the ET-50 as the ionic conductivity of the latter is 20 times higher. Moreover, this potential rapidly increases with the cycles (Figure 6-D). The evolution of the overpotential with the cell cycling is shown in the Figure 6. Although it shows the highest overpotential, ET-0 has better cycling stability with 98 cycles whereas the ET-30 and ET-50 work for 69 and 18 cycles respectively. The overpotential of ET-0 is the highest observed at the first cycle and the charge voltage increases rapidly to 4.35 V vs. Li^+/Li after only 12 cycles. On the other hand, the ET-30 shows charge voltage below 4.35 V vs. Li^+/Li until the 54th cycle. As shown previously, the addition of EMI TFSI enables to increase the ionic conductivity of the electrolyte but it may also enhance the O_2 solubility.[21,22] Thus a better reversibility is observed for the electrolytes containing the ionic liquid for the first cycles.

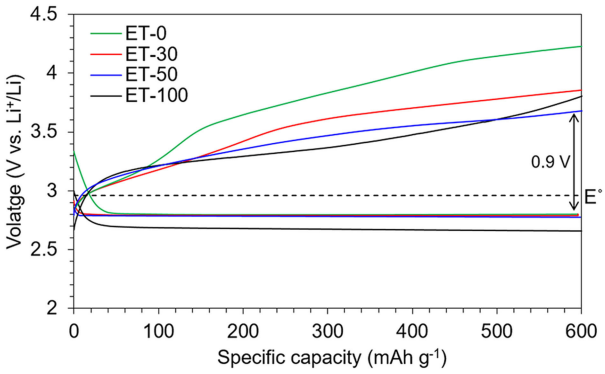

Figure 5. First cycle galvanostatic discharge and recharge of Li–O_2 cell at 25 °C with the different electrolytes studied, at the applied current of 200 mA g^{-1} and limited capacity of 600 mAh g^{-1}.

Indeed, the charge potential increases with the number of cycles until the battery fails, which occurs earlier when the electrolyte contains EMI TFSI. This can be ascribed to the degradation products formation which was proved in previous work, that it is faster in presence of EMI TFSI than in DMSO without RTIL.[23] It was observed indeed that with cycling, LiOH concentration increases more rapidly in presence of ionic liquids, due to the high reactivity of the C2 proton of imidazolium cations. Moreover, Das *et al.*[7] exlpained that imidazolium-based cations are unstable in presence of radical peroxide.[24] Then, even with a reduced overpotential, so a more reversible battery reaction, the electrolyte degradation is more important in presence of the RTIL. Concerning the DMSO, Sharon *et al.*[25] observed the formation of side products when exposed to superoxide. This would explain the battery cycling being limited at 98 cycles when using the ET-0.

In summary, it is important to remark that for blended DMSO/EMI TFSI electrolytes, significant improvements are observed concerning the thermal stability and cell overpotential. In particular, by adding 30% in weight of EMI TFSI, the degradation/evaporation occurs at a temperature 80° higher and the ionic conductivity increasing from 7.88 to 13.1 mS cm^{-1}. The Li-O_2 battery performance is also improved with a 35% higher full discharge capacity and an overpotential reduced to 1.06 V versus 1.43 V for the DMSO electrolyte. Reasonable cycling performance are also obtained, although the electrolyte without RTIL shows higher cycling life (98 cycles), 69 cycles are obtained with the blended electrolyte. The use of a RTIL more stable against peroxide radical attack and in presence of lithium may enable a longer cycle life. Besides, this study shows that the bulk electrolyte parameters (ionic conductivity, viscosity) have more influence on the battery performance than the cathode surface parameters (cell overpotential, wettability) and the anode surface parameters (Li/Li overpotential).

Experimental Section

EMI TFSI was purchased from Solvionic and DMSO from Sigma Aldrich. Both are used after drying with 4 Å molecular sieves (Aldrich) for two days. Lithium perchlorate salt was purchased from Sigma Aldrich, dry with purity of 99.99%. Four mixed electrolytes ET-0, ET-30, ET-50 and ET-100 are prepared by adding 5 w% of $LiClO_4$ to the mixed solution of DMSO and EMI TFSI in a glove box filled with purified argon. The weight ratio of EMI TFSI/DMSO in ET-0, ET-30, ET-50 and ET-100 are 0/100, 30/70, 50/50 and 100/0 respectively. The water content of the electrolytes prepared is measured by Karl Fischer (Coulometer KF 831) titration and was determined to be less than 50 ppm.

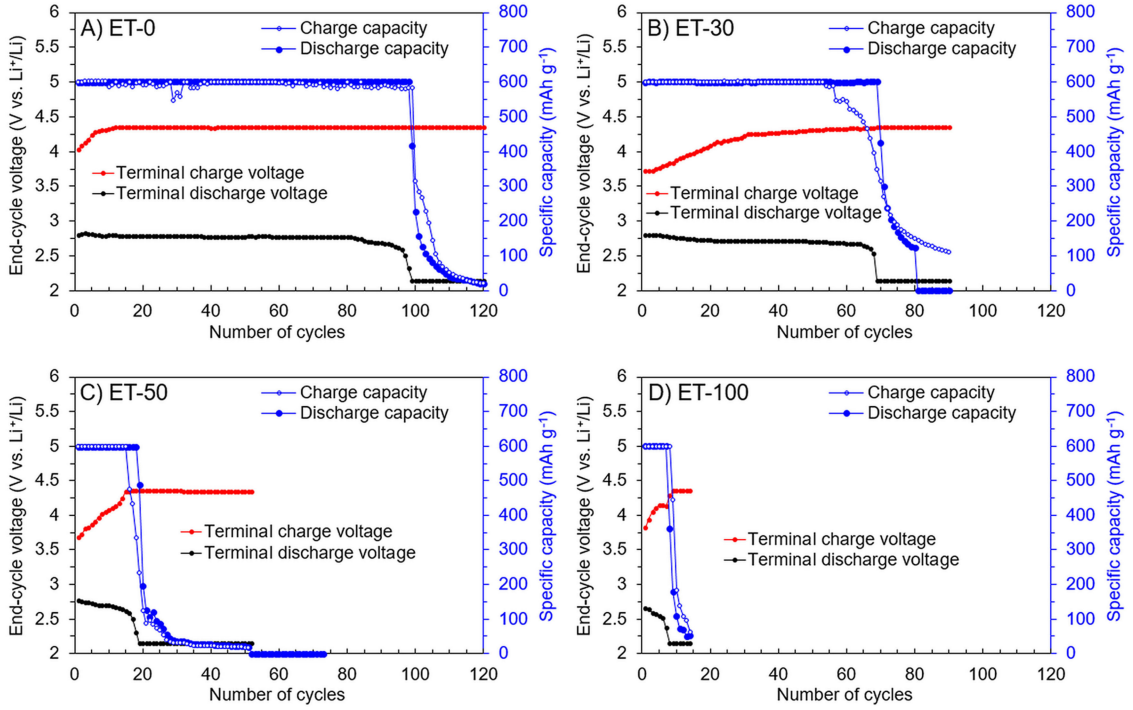

Figure 6. Cycling performance (blue curves) and corresponding cell-voltage cut-off (red and black curves) of Li–O_2 cells at 25 °C with A) ET-0, B) ET-30, C) ET-50 and D) ET-100 electrolytes at a constant current of 200 mA g^{-1} and 600 mAh g^{-1} capacity limit.

The ionic conductivity is measured with a titanium tip (Ref. 50, 73) on an EC Meter Basic 30+ conductimeter (Crison Instrument) at room temperature. The viscosities are measured using a Malvern Bohlin CVO 100–901 rheometer in air, at room temperature. Shear rates are varied between 0.1 s^{-1} and 10 s^{-1}. No shear thinning behavior due to the variation of the shear rate is observed. Hence, the viscosities are determined from the plateau value at all shear rates. Differential scanning calorimetry (DSC) results are obtained using a TA Instruments Q20 apparatus. Samples weighting 5–14 mg are hermetically sealed in aluminum pans and cooled to −90 °C followed by heating to 200 °C applying a scan rate of 10 °C min^{-1}. Finally, the samples are cooled back to −90 °C at the same scan rate.

Lithium/lithium stripping/plating tests are carried out in CR2032 coin cells using lithium chip (Ref: EQ-Lib-LiC25, MTI Corp.) as anode and cathode and a glass fiber membrane (Whatman GF/A) as separator. A quantity of 150 µL of each electrolyte is used to perform the galvanostatic cycling test with an applied current of 10 mA cm^{-2} with limited charge/discharge time of one hour and a cut-off voltage limit of +/−1 V vs. Li^+/Li.

Li–O_2 batteries are assembled inside an Ar-filled glove box using ECC-air cell (EL Cell). The cathode for the Li–O_2 battery are prepared from a mixture of 90 wt% TIMCAL Super C65 and 10 wt% polyvinylidene fluoride (PVdF Kynar ADX 161, Arkema) in N-methyl-2-pyrrolidone (NMP, 99.5 %, Sigma-Aldrich). The slurry is tape casted on a Gas Diffusion Layer (GDL SIGRACET 24BC – SGL Company) using the doctor blade technique up to an active loading of 1.5 mg cm^{-2}. Although this GDL may participate to the overall capacity of the battery,[26] only the mass of TIMCAL is taken into account to normalize the specific capacity calculated. A circular lithium chip (Ref: EQ-Lib-LiC25, MTI Corp.) is used as the anode. The separator is a glass fiber membrane (Whatman GF/A) soaked with the tested electrolyte. Prior applying any current, the cell is maintained under O_2 flow (8 mL min^{-1}) up to stabilize the open circuit voltage after 10 hours. Galvanostatic cycling tests are performed at 25 °C using a VMP3 Biologic instrument with a current of 200 mA g^{-1} applied between 2.15 V and 4.35 V vs. Li^+/Li as cut-off voltage with an oxygen flow rate of 8 mL min^{-1} and discharge/recharge cycle duration of 6 h each.

Acknowledgements

The STABLE project received funding from the European Union's FP7 research and innovation program under grantagreement N° 314508. G. G. thanks financial support from project CTQ2015-65439-R from the MINECO.

Conflict of Interest

The authors declare no conflict of interest.

Keywords: electrolytes · energy storage · ionic liquids · lithium-oxygen batteries · thermal stability

[1] G. Girishkumar, B. D. McCloskey, A. C. Luntz, S. Swanson, W. Wilcke, *J. Phys. Chem. Lett.* **2010**, *1*, 2193–2203.
[2] C. J. Allen, J. Hwang, R. Kautz, S. Mukerjee, E. J. Plichta, M. a. Hendrickson, K. M. Abraham, *J. Phys. Chem. C* **2012**, *116*, 20755–20764.
[3] S. Ferrari, E. Quartarone, C. Tomasi, M. Bini, P. Galinetto, M. Fagnoni, P. Mustarelli, *J. Electrochem. Soc.* **2014**, *162*, A3001–A3006.
[4] M. Olivares-marín, A. Sorrentino, E. Pereiro, D. Tonti, *J. Power Sources* **2017**, *359*, 234–241.
[5] G. A. Elia, J. Hassoun, B. Scrosati, F. Mueller, D. Bresser, S. Passerini, P. Oberhumer, N. Tsiouvaras, J. Reiter, *Nano Lett.* **2014**, *14*, 6572–6577.

[6] D. Bresser, E. Paillard, S. Passerini, *J. Electrochem. Sci. Technol.* **2014**, *5*, 37–44.
[7] S. Das, J. Højberg, K. B. Knudsen, R. Younesi, P. Johansson, P. Norby, T. Vegge, *J. Phys. Chem. C* **2015**, *119*, 18084–18090.
[8] S.-M. Han, J.-H. Kim, D.-W. Kim, *J. Electrochem. Soc.* **2015**, *162*, A3103–A3109.
[9] Y. Li, Z. Zhang, D. Duan, Y. Sun, G. Wei, X. Hao, S. Liu, Y. Han, W. Meng, *J. Power Sources* **2016**, *329*, 207–215.
[10] P. Lou, C. Li, Z. Cui, X. Guo, *J. Mater. Chem. A* **2016**, *4*, 241–249.
[11] W. Ni, S. Liu, Y. Fei, Y. He, X. Ma, L. Lu, Y. Deng, *ACS Appl. Mater. Interfaces* **2017**, *9*, 14749–14757.
[12] S. Matsuda, K. Uosaki, S. Nakanishi, *J. Power Sources* **2017**, *356*, 12–17.
[13] H. Nakamoto, Y. Suzuki, T. Shiotsuki, F. Mizuno, S. Higashi, K. Takechi, T. Asaoka, H. Nishikoori, H. Iba, *J. Power Sources* **2013**, *243*, 19–23.
[14] K. Cai, H. Jiang, W. Pu, *Int. J. Electrochem. Sci.* **2014**, *9*, 390–397.
[15] L. Cecchetto, M. Salomon, B. Scrosati, F. Croce, *J. Power Sources* **2012**, *213*, 233–238.
[16] C. O. Laoire, S. Mukerjee, K. M. Abraham, E. J. Plichta, M. a. Hendrickson, *J. Phys. Chem. C* **2009**, *113*, 20127–20134.
[17] P. Bonhôte, A.-P. Dias, N. Papageorgiou, K. Kalyanasundaram, M. Grätzel, *Inorg. Chem.* **1996**, *35*, 1168–1178.
[18] L. Grande, E. Paillard, G. T. Kim, S. Monaco, S. Passerini, *Int. J. Mol. Sci.* **2014**, *15*, 8122–8137.
[19] G. B. Appetecchi, S. Scaccia, S. Passerini, **2000**, *147*, 4448.
[20] M. Roberts, R. Younesi, W. Richardson, J. Liu, J. Zhu, K. Edstr, *Electrochem. Lett.* **2014**, *3*, A62–A65.
[21] Y.-F. Hu, Z.-C. Liu, C.-M. Xu, X.-M. Zhang, *Chem. Soc. Rev.* **2011**, *40*, 3802.
[22] S. Monaco, A. M. Arangio, F. Soavi, M. Mastragostino, E. Paillard, S. Passerini, *Electrochim. Acta* **2012**, *83*, 94–104.
[23] E. Knipping, C. Aucher, G. Guirado, F. F. Fauth, L. Aubouy, *New J. Chem.* **2017**, *41*, 7267–7272.
[24] M. Hayyan, F. S. Mjalli, M. A. Hashim, I. M. Alnashef, *J. Mol. Liq.* **2013**, *181*, 44–50.
[25] D. Sharon, M. Afri, M. Noked, A. Garsuch, A. A. Frimer, D. Aurbach, *J. Phys. Chem. Lett.* **2013**, *4*, 3115–3119.
[26] J. Zeng, J. R. Nair, C. Francia, S. Bodoardo, N. Penazzi, *Solid State Ionics* **2014**, *262*, 160–164.

Manuscript received: August 9, 2018
Version of record online: November 5, 2018